JOURNAL OF APPLIED ELECTROCHEMISTRY 11 (1981) 417–422

Some aspects of the electrochemical response of iron hydroxide precipitated on different conducting substrates

V. A. MACAGNO, J. R. VILCHE, A. J. ARVIA

División Electroquímica, Instituto de Investigaciones Fisicoquímicas Teóricas y Aplicadas (INIFTA), Sucursal 4, Casilla de Correo 16, 1900 La Plata, Argentina

Received 28 July 1980

The potentiodynamic behaviour of different conducting substrates (Pt, Au and vitreous carbon) covered with iron hydroxide formed by colloidal precipitation in 0.01 M NaOH is investigated in the potential range associated with the electrochemical stability of water at 25° C. The electrochemical characteristics are mainly related to the $Fe(OH)_2/FeOOH$ redox couple formed from both thin and thick iron hydroxide layers. The results can be interpreted through the complex reaction pattern already discussed for the electrochemical behaviour of Fe in alkaline solutions.

1. Introduction

The electrochemical study of interphases of the type conducting material/nonmetal phase/electrolyte is of growing interest because of their significance both in fundamental and applied electrochemistry [1–14]. Thus the electronic structure of the oxide and hydroxide layers is involved in the corrosion and passivity characteristics of the base material and can also influence the rate and mechanism of electrochemical reactions. On the other hand, under other conditions the layer may participate in relatively fast redox processes.

Previous results obtained for the $Ni(OH)_2$/NiOOH redox couple formed on different conducting substrates covered with nickel hydroxide produced by colloidal precipitation [12, 13] suggest the possibility of obtaining a comparable electrochemical response from conducting substrates covered with iron hydroxide. The separation of the various reactions contributing to the corrosion and passivation of iron in alkaline electrolytes can be attempted after evaluation of the electrochemical characteristics of iron hydroxide.

2. Experimental

The $M/Fe(OH)_2$ working electrodes were prepared on the following conducting substrates (M): a vitreous carbon disc (Union Carbide, low density, 0.071 cm^2), pure gold wire (99.99%, 0.24 cm^2) and platinum wire (Johnson, Matthey and Co., spectroscopic quality, 0.27 cm^2). The cleaning of both Au and Pt consisted of 15 min immersion in a 1 : 1 H_2SO_4/HNO_3 mixture, 5 min immersion in water followed by abundant rinsing in triply distilled water. The vitreous carbon was first polished with finest-grade emery paste, then cleaned by immersion in boiling diluted HCl and finally thoroughly rinsed in triply distilled water.

The precipitation of iron hydroxide on the different substrates was made at 25° C using a standardized procedure. This consisted of 5 to 25 alternate immersions in an alkaline solution (0.01 M NaOH + 0.66 M Na_2SO_4) and an Fe(II) solution (4×10^{-3} M $FeSO_4$). The immersion time in each solution was fixed at 5 s.

The iron hydroxide working electrode was placed in a conventional three-compartment Pyrex glass cell using the 0.01 M NaOH + 0.66 M Na_2SO_4 electrolyte solution. The counter electrode was made from a large Pt sheet. The potential of the working electrode was measured against a properly shielded saturated calomel electrode (SCE). Runs were made at 25° C under purified N_2 gas saturation. The different electrochemical interphases were perturbed with repetitive triangular potential sweeps (RTPS) initiated towards the positive potential side within preset cathodic

0021–891X/81/040417–06$02.60/0

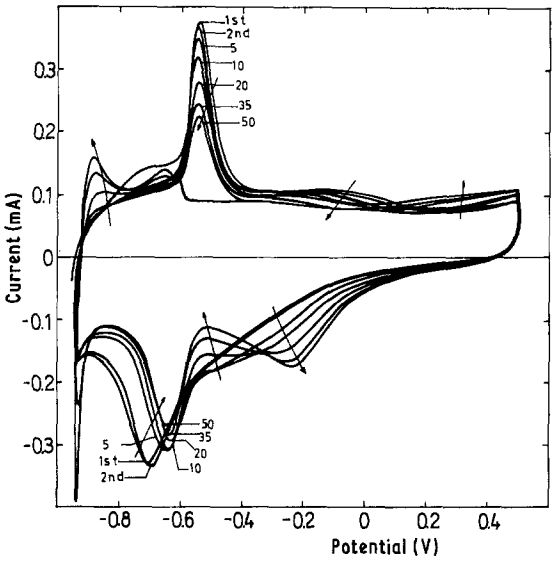

Fig. 1. Potentiodynamic E–I displays (RTPS) run at 0.2 V s^{-1} from $E_{s,c} = -0.94$ V onwards with a Pt/$Fe(OH)_2$/electrolyte interphase prepared by five alternate immersions of 5 s each. The first, the second and the E–I profiles after 5, 10, 20, 35 and 50 min cycling are depicted.

($E_{s,c}$) and anodic ($E_{s,a}$) switching potentials at the potential sweep rate (v) of 0.2 V s^{-1}.

3. Results

The complexity of the potentiodynamic potential–current (E–I) displays obtained on the different substrates depends on $E_{s,c}$, $E_{s,a}$, the number of RTPS and the nature of the substrate (Figs. 1 and 2). The anodic current peak which appears in the −0.4 V to −0.5 V range is associated with the Fe(II) to Fe(III) electro-oxidation while that located in the −0.7 V to −0.6 V range is related to the reverse reaction [15, 16]. The charge, which can be calculated from the potentiodynamic E–I profiles, changes during the RTPS and depends on $E_{s,c}$ and $E_{s,a}$ because of the extent of the electro-oxidation and electro-reduction of the gold or platinum surface. The thickness of the iron hydroxide layer varied from submonolayer to multilayer, as deduced by comparing the charge with that involved in the O-electrosorption and O-electrodesorption of the conducting substrates (either Pt [17, 18] or Au [19, 20].

The potentiodynamic E–I display shown in Fig. 1 corresponds to the initial Pt/iron hydroxide/alkaline solution interphase. The initial iron hydroxide layer thickness is of the order of one monolayer, calculated as 1.8 nm mC^{-1} cm^2 [11]. Its potentiodynamic behaviour can be described by comparing the E–I display with that of the Pt/0.01 M NaOH interphase [17, 18] perturbed under the same conditions. During the initial anodic potential excursion between −0.95 V and 0.5 V the anodic current peak at −0.55 V is preceded by a limiting current which extends from −0.65 V upwards. In the potential range −0.2 V to 0 V, where the electro-oxidation of Fe(II) species is feasible, a broad and poorly defined anodic current peak is found. During the RTPS, the E–I profile approaches a complex current plateau from −0.4 V up to 0.4 V which is mainly related to the O-electrosorption on Pt [17, 18].

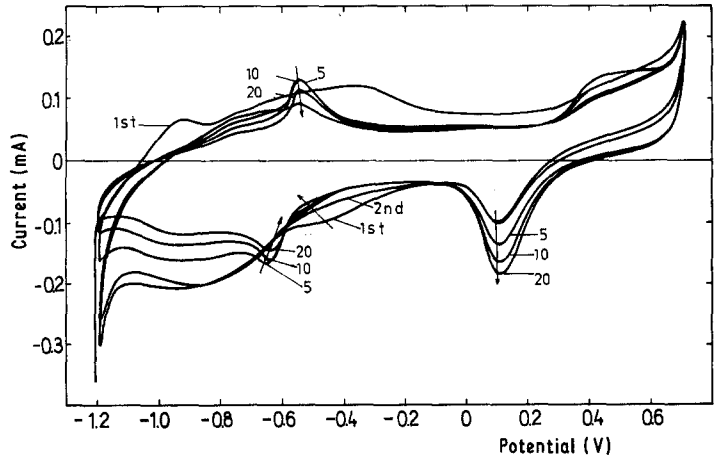

Fig. 2. Potentiodynamic E–I diplays (RTPS) run at 0.2 V s^{-1} from $E_{s,c}$ = −1.2 V onwards with an Au/$Fe(OH)_2$/electrolyte interphase prepared by five alternate immersions of 5 s each. The first, the second and the E–I profiles after 5, 10 and 20 min cycling are shown.

The returning potential excursion exhibits a cathodic contribution increasing from −0.2 V up to −0.5 V which corresponds to the O-electrodesorption from Pt [17, 18]. The latter precedes the cathodic current peak at approximately −0.6 V, which is related to the Fe(III) to Fe(II) electroreduction [15, 16]. At approximately −0.9 V hydrogen discharge from water takes place. Continued potential cycling produces a progressive decrease in the charge related to the Fe(II)/Fe(III) redox reactions and simultaneously an increasing contribution of both the O-electrosorption and O-electrodesorption and the H-electroformation and H-electro-oxidation on Pt. The direction of these changes is indicated by the arrows shown in Fig. 1. The appreciable initial inhibition of both processes disappears gradually during potential cycling. Likewise, a progressive shift of the current peak associated with the electroreduction of the Fe(III) species towards more positive potentials during the RTPS is noticed. The remarkable overlapping of the various reactions makes Pt a relatively poor substrate to study the electrochemical reactions related to the iron hydroxide.

The complex potentiodynamic *E–I* display resulting from the initial Au/iron hydroxide interphase (Fig. 2) can also be analysed by comparison with the corresponding potentiodynamic *E–I* profile of the Au/0.1 M NaOH interphase [19, 20]. The RTPS *E–I* profiles in the −1.2 V to 0.7 V range (Fig. 2) can be divided into two main regions, namely, one from −1.0 V to −0.1 V, which is principally related to the Fe(II)/Fe(III) redox process, and another from −0.1 V to 0.6 V which covers the O-electrosorption/O-electrodesorption on Au. At the highest negative potentials a contribution from the H_2 evolution current is also observed. Similarly, at the highest positive potentials, the O_2 evolution region is reached.

During the first triangular potential sweep the *E–I* profile is remarkably different from later ones, especially in the potential range where the Fe(II)/Fe(III) reactions take place. Furthermore, the anodic and cathodic current peaks related to the overall reaction become better defined after 5 min of RTPS when the $E_{s,c}$ value is in the H_2 evolution potential range and the $E_{s,a}$ value is in the O_2 evolution potential region. On further extending the duration of the RTPS there is a slight decrease in the heights of the anodic and cathodic current peaks related to the Fe(II)/Fe(III) electrochemical reactions together with a simultaneous increase in the current contributions related to the O-electrosorption/O-electrodesorption.

The negative-going *E–I* profiles depicted in Fig. 2 are to some extent influenced by the slight amount of O_2 which is formed beyond 0.6 V. It appears that the efficiency of the O_2 evolution reaction decreases during the RTPS. This occurs simultaneously with the increase of the O-electrodesorption current peak and the decrease of the O_2 electroreduction current which is observed in the 0.6 V to −1.0 V range. This effect is apparently accompanied by the decrease of the H_2-evolution current during the RTPS.

The preceding analysis suggests that the isolation of the overall Fe(II)/Fe(III) redox processes from other electrochemical processes occurring on Au can be achieved by confining the potential sweep range between −1.0 V and 0.0 V (Fig. 3). Thus, as the switching potential range is restricted (Fig. 3a), the anodic to cathodic charge ratio along the potential cycling always remains practically equal to one. However, during the initial potential cycles two conjugated redox couples can be distinguished, one in the −0.8 V range which is less clear than the one located between −0.6 V to −0.7 V. The current peaks of the latter are clearly noticeable. During the RTPS the contribution of the former redox system decreases while that of the second one increases slightly and shifts towards positive potentials. A reasonably stable *E–I* profile then results after 5 min RTPS.

The composite structure of the current peaks related to the Fe(II)/Fe(III) redox system can be depicted by perturbing the interphase with potential sweeps involving gradually changing switching potentials (either $E_{s,a}$ or $E_{s,c}$) after the stabilized RTPS *E–I* profile has been reached (Figs. 3b and c). In this way, a clear splitting of both the anodic and cathodic current peaks is observed.

Thicker iron hydroxide layers under comparable perturbation conditions (Fig. 4) exhibit similar features to those already described for thin films, but for the latter the charge decreases during cycling. The charge decrease can be due to: (a) the lack of saturation of the electrolyte with the $Fe(OH)_2$ species; (b) mechanical detachment from the substrate; and (c) a partial transformation of

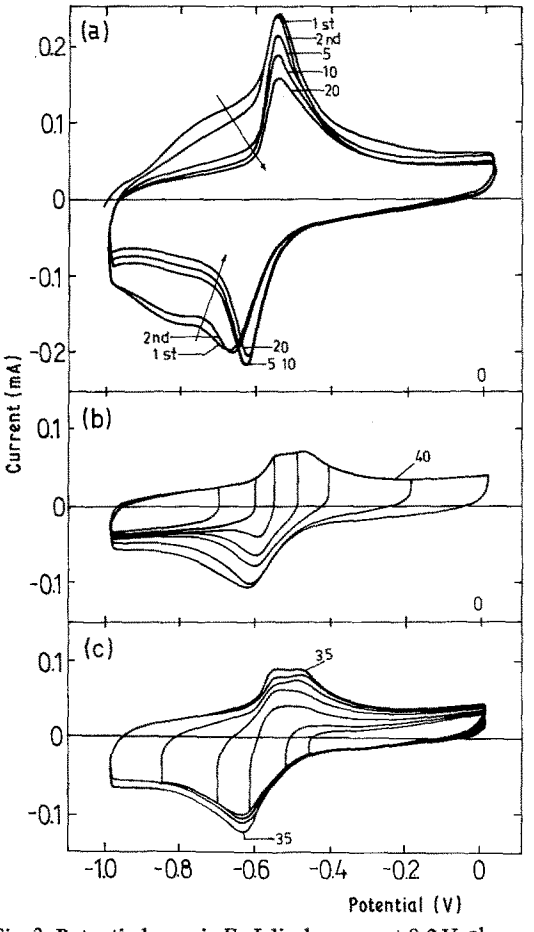

Fig. 3. Potentiodynamic E–I displays run at 0.2 V s^{-1} between −1.0 V and 0 V with an Au/$Fe(OH)_2$/electrolyte interphase obtained as indicated in Fig. 2. (a) E–I profiles (RTPS) initiated from −1.0 V onwards. The first, the second and the E–I profiles after 5, 10 and 20 min cycling are depicted. (b) Influence of changing $E_{s,a}$ on the E–I display resulting after 40 min RTPS. (c) Influence of changing $E_{s,c}$ on the E–I display resulting after 35 min RTPS.

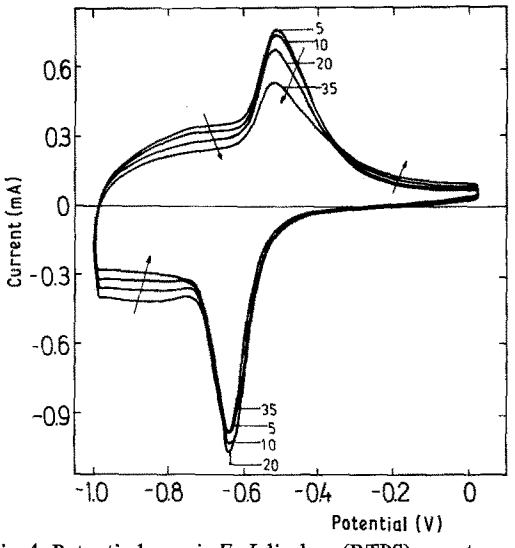

Fig. 4. Potentiodynamic E–I displays (RTPS) run at 0.2 V s^{-1} with an Au/$Fe(OH)_2$/electrolyte interphase obtained from 25 alternate immersions of 5 s each. The changes in the E–I profile during the RTPS are indicated by arrows.

the Fe(III) species into one which is non-electroreducible in the potential range of the experiments.

The behaviour of the vitreous carbon/iron hydroxide/alkaline solution interphase is much simpler than the behaviour of those previously described (Fig. 5). Under the RTPS perturbation the E–I display can be described in the same way as those obtained with Au in the restricted potential range. The experiment on vitreous carbon definitely shows that the current contributions related to the Fe(II)/Fe(III) system are located in a wide potential range extending roughly from −0.8 V to −0.2 V. The electrochemical characteristics of the initial E–I display exhibit a remarkable polarization which decreases on further potential cycling. This effect is accompanied by appreciable current contributions, both anodic and cathodic, at the negative potential side of the corresponding current peaks.

4. Discussion

In the alkaline electrolyte the initial layer of iron hydroxide is electro-oxidized to FeOOH species. The overall reaction occurring in the −0.8 V to 0.2 V potential range can be formally written in one of the following ways:

$$Fe(OH)_2 = FeOOH + H^+ + e \quad (1a)$$

$$Fe(OH)_2 + OH^- = FeOOH + H_2O + e. \quad (1b)$$

The overall electrochemical reaction, which involves a relatively fast proton transfer process, takes place practically independently of the underlying conducting material, which can be either Hg [23], Fe [16], Pt, Au or vitreous carbon. The potentiodynamic current peaks related to Reaction 1 are unambiguously established when substrates other than Fe are used.

The separation of the current peak potential related to the $Fe(OH)_2$/FeOOH redox reactions in vitreous carbon is far too large to be explained

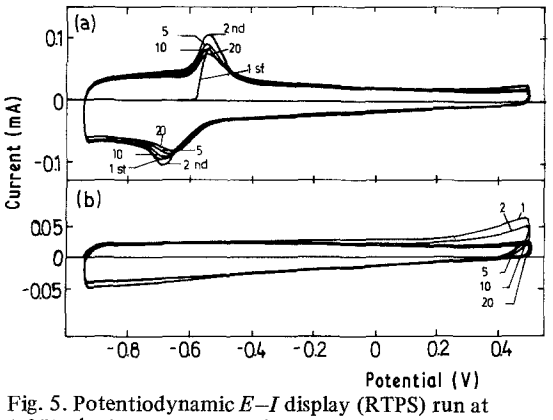

Fig. 5. Potentiodynamic E–I display (RTPS) run at 0.2 V s^{-1} with a C(vitreous)/$Fe(OH)_2$/electrolyte interphase obtained from 5 alternate immersions of 5 s each. (a) The first, the second and the E–I profiles after 5, 10 and 20 min RTPS are shown. (b) Blank.

through a single reversible electrochemical process in a reacting film. The broad current peaks involved in the redox processes suggest an interpretation of the electrochemical reaction in terms of a complex reaction pattern involving structural changes occurring simultaneously with the electrochemical reactions, as has been advanced for both Ni and Fe electrodes in alkaline solutions [24–26]. In this sense, the electrochemical behaviour of the vitreous carbon/iron hydroxide interphase is comparable to that of the vitreous carbon/nickel hydroxide interphase [13].

Both on Pt and Au the O-electrosorption/O-electrodesorption processes are observed at potentials more positive than the potential range of Reaction 1 so that at potentials reaching the potential range of the $Fe(OH)_2$/FeOOH electrochemical reaction the structures of the corresponding interphases should be represented by a scheme such as M/M(O)/iron hydroxide where M stands for the base metal and (O) corresponds to the O-electrosorbed layer without stoichiometry compromise. In this case, the electrochemical reactions related to the two layers behave as separate layers so that probably no mixed oxide species are formed.

Comparison of the electrochemical behaviour of the M/iron hydroxide and M/nickel hydroxide interphases under the same type of potential perturbation and at the same temperature shows remarkable differences between Pt and Au substrates. For both metals, the $Fe(OH)_2$/FeOOH redox process occurs at potentials lower than those of the O-electrosorption/O-electrodesorption reactions, in contrast with the results already reported for the $Ni(OH)_2$/NiOOH redox process [12, 13]. Hence, in principle, it is reasonable to expect that the degree of interaction between the reactions occurring at the two layers becomes greater in the M/iron hydroxide interphase than in the M/nickel hydroxide interphase. On the other hand, the changes of the potentiodynamic E–I display obtained with both the Pt/iron hydroxide and Au/iron hydroxide interphases show a gradual replacement of the iron hydroxide layer by either Pt(O) or Au(O) layers respectively during cycling. This indicates that the O-layers both in Pt and Au are more tightly bound to the surface than the iron hydroxide layer. The interaction between the electrochemical reactions at the two layers is more remarkable for Pt than for Au because the potential range of the overall processes for the former is smaller than for the latter. This interaction becomes more evident when the charges playing part in the sandwich-type electrode are of the order of one monolayer thickness. For Pt the interaction also reflects the apparent increase of the electrocatalytic activity of the substrate for the hydrogen electrode reaction. Simultaneously, the contribution of the O-electrosorption/O-electrodesorption process progressively increases.

The current peak multiplicity of the potentiodynamic response of the $Fe(OH)_2$/FeOOH redox couple may be accounted for in terms of time effects related to the molecular structure of iron hydroxide [27–29]. The ageing of the latter implies either an increase of the molecular weight of the basic polymeric unit or a decrease of the Fe(III) fraction available for electroreduction. This supports the interpretation that various $Fe(OH)_2$ and FeOOH species may participate in the electrochemical reactions, as was suggested earlier for the $Ni(OH)_2$/NiOOH redox system [24, 25]. The ageing effect may be caused mainly by a slow transformation of hydroxo-type into oxo-type bridges in the polymer.

Acknowledgements

INIFTA is sponsored by the Consejo Nacional de Investigaciones Científicas y Técnicas, the Universidad Nacional de La Plata and the Comisión de Investigaciones Científicas (Provincia

de Buenos Aires). This work was partially supported by the Regional Program for the Scientific and Technological Development of the Organization of the American States. One of us (VAM) thanks the University of Córdoba for leave of absence.

References

[1] M. Nagayama and M. Cohen, *J. Electrochem. Soc.* **109** (1962) 781.
[2] *Idem, ibid* **110** (1963) 670.
[3] M. Markovac and M. Cohen, *ibid* **114** (1967) 674, 678.
[4] K. J. Vetter, *Electrochim. Acta* **16** (1971) 1923.
[5] J. L. Leibenguth and M. Cohen, *J. Electrochem. Soc.* **119** (1972) 987.
[6] M. M. Lohrengel and J. W. Schultze, *Electrochim. Acta* **21** (1976) 957.
[7] U. Stimming and J. W. Schultze, *Ber. Bunsenges. Phys. Chem.* **80** (1976) 1297.
[8] R. S. Sapieszko, R. C. Patel and E. Matijevic, *J. Phys. Chem.* **81** (1977) 1061.
[9] R. Babic and B. Lovrecek, *Elektrokhim.* **15** (1979) 16.
[10] M. Sakashita and N. Sato, *Corrosion* **35** (1979) 351.
[11] M. M. Lohrengel, P. K. Richter and J. W. Schultze, *Ber. Bunsenges. Phys. Chem.* **83** (1979) 490.
[12] M. E. Folquer, J. R. Vilche and A. J. Arvía, *J. Electrochem. Soc* **127** (1980) 2634.
[13] V. A. Macagno, J. R. Vilche and A. J. Arvía, to be published.
[14] J. R. Vilche and A. J. Arvía, *Lat. Amer. J. Chem. Eng. Appl. Chem.* **9** (1979) 35.
[15] D. Geana, A. A. El Miligy and W. J. Lorenz, *J. Appl. Electrochem.* **4** (1974) 337.
[16] R. S. Schrebler Guzmán, J. R. Vilche and A. J. Arvía, *Electrochim. Acta* **24** (1979) 395.
[17] H. Angerstein-Kozlowska and B. E. Conway, *J. Electroanal. Chem.* **95** (1979) 1.
[18] M. Y. Duarte, M. E. Martins and A. J. Arvía, *Anal. Quim. (Espana)*, in press.
[19] R. Cordova, M. E. Martins and A. J. Arvía, *J. Electrochem. Soc.* **126** (1979) 1172.
[20] *Idem, Electrochim. Acta* **25** (1980) 453.
[21] G. Bianchi, F. Mazza and T. Mussini, *Electrochim. Acta* **11** (1966) 1509.
[22] R. W. Zurilla, R. K. Sen and E. Yeager, *J. Electrochem Soc.* **125** (1978) 1103.
[23] J. O'M. Bockris and Z. Nagy, *J. Chem. Educ.* **50** (1973) 839.
[24] R. S. Schrebler Guzmán, J. R. Vilche and A. J. Arvía, *J. Appl. Electrochem.* **9** (1979) 183.
[25] R. S. Schrebler Guzmán, J. R. Vilche and A. J. Arvía, *ibid* **9** (1979) 321.
[26] J. R. Vilche and A. J. Arvía, *Acta Científica Venezuela*, in press.
[27] G. Nembrini, J. Buffle and W. Haerdi, *J. Colloid Interface Sci.* **57** (1976) 327.
[28] J. Buffle and G. Nembrini, *J. Electroanal. Chem.* **76** (1977) 101.
[29] E. Matijevic and P. Scheiner, *J. Colloid Interface Sci.* **63** (1978) 509.